Baltic Astronomy, vol.4, 270–301, 1995.

G 29–38 AND ASTEROSEISMOLOGY OF THE COOL DAV WHITE DWARFS

S. J. Kleinman

Department of Astronomy, University ot Texas, Austin, TX 78712, U.S.A.

Received September 1, 1995.

Abstract. After gathering many seasons of data on G 29-38, I find, amongst a plethora of linear combination modes, an underlying stable set of normal $l = 1$ g-modes, ripe for asteroseismological plucking. I have also found multiplets in the star's FTs, but with unexplained peculiarities. I also report on observations of three other cool DAVs whose class properties support the G 29-38 results and the results of Clemens (1993, 1994) from the hotter DAVs. I find the cool DAVs are also remarkably similar as a class, sharing many common modes of oscillation.

Key words: stars: interiors – stars: oscillations – stars: individual: G 29-38

1. The pulsation spectrum of G 29-38

1.1. The ensemble approach

Of all the variable white dwarfs, the DAVs have been the hardest to study with asteroseismology. The hotter DAVs have only a few modes – too few to make a believable mode identification. The cooler DAVs show many modes, but most are unstable and many are combination modes (modes whose frequencies are linear combinations of other modes) which greatly complicate mode identification. Clemens (1993, 1994) showed that by treating the ensemble of the hot DAVs as a single star, he could make consistent mode identifications. Here, I will use data from many different observing seasons on G 29-38 to search for normal modes. Where Clemens used many different stars, I will use many different observing seasons. The goals, however, are similar: search the resulting set of modes for a sensible set of normal mode oscillations.

G 29-38's power spectra change dramatically from year to year, with less dramatic changes occurring even during a given season. If the star oscillates in normal g-modes, but picks and chooses which particular modes to oscillate in at any given time, we should see modes that recur and definite gaps where no normal modes ever appear. Amidst the wealth of modes that come and go with each observing season, we are searching for an underlying stable structure that might shed some light on the nature of the variations. Unfortunately, with the richness of the g-mode spectra, we can get a mode just about anywhere; as long as we remain in model space, we can simply choose from an infinite (although discrete) set of l, k and m values to get a mode nearly anywhere we want. Fortunately, however, the stars are simpler than our models, seeming only to select modes with l less than 3.

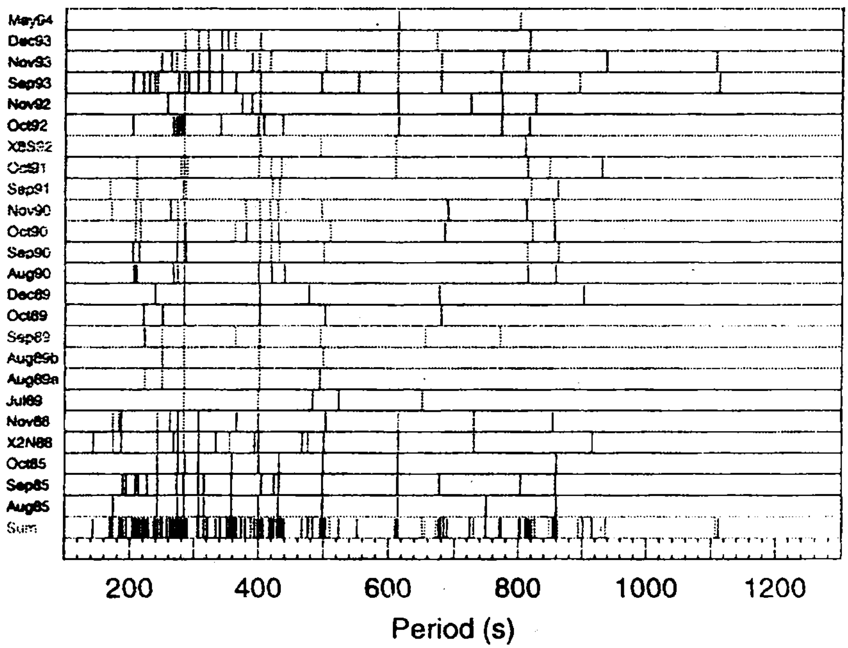

Fig. 1. Schematic diagram of G 29-38's periodicities for the entire data set.

Fig. 1 is a schematic mode plot for our G 29-38 data. The amplitude information has been ignored here and every mode is plotted with the same amplitude to better highlight the possible groupings. Note the X-axis is period, not frequency. A wealth of information is contained within this plot, but for now, note the bottom *Sum* panel and the conspicuous lack of groupings. The obvious conclusion here is that the modes we see are not explainable by single-l, normal-mode pulsations. While there appear to be some gaps in G 29-38 's schematic mode plot, there are few concise groupings.

Since it is already known that this star (and others of its class) have linear combination modes, we will start by removing the linear combinations and see what the remaining modes look like. If we are indeed seeing normal g-mode pulsations, we expect to find series of nearly equally spaced periodicities, representing a succession of different-k, same-l modes. If there is more than one l present, we expect to see two such patterns. More likely, however, is a set of $l = 1$ only pulsations with perhaps, but not necessarily, a mode or two of $l = 2$. The simplest approach is to assume only $l = 1$ modes and see what, if anything, cannot be explained as either an $l = 1$, or a linear combination mode.

Our ability to identify (and hence remove) the linear combinations depends greatly on the signal to noise ratio and the resolution of each transform. To help avoid uncertain and incorrect identifications, I now restrict my analysis to the best data sets available – one per year: Aug85 is the August 1985 data set from a combined campaign by South Africa and McDonald observatories. X2N88 is the data from the WET XCOV2 campaign on G 29–38 in November 1988. Sep89 is a 20-night data set from McDonald from September 1989. Oct90 and Sep93 are also single-site data sets from the McDonald Observatory during October 1990 and September 1993, respectively. X8S92 is the data from the second WET run (XCOV8) on G 29-38 in September 1992.

Fig. 2 is the schematic period diagram minus the identified linear combinations from this selected data subset. This new schematic period diagram is substantially cleaner and qualitatively shows the mode groupings we would expect for normal-mode pulsations. The roughly equally-spaced groups seen in the *Sum* row suggest a mean period of roughly 50 s. We see a near complete set of modes from 110 s to 900 s with two more at longer periods. With few exceptions, the groups are tight and have distinct gaps between them.

The data from September, 1993 have the most modes and nicely reproduce the expected ≈ 50 s spacing. This season is unique in that there appear to be six consecutive k values in one period range. The

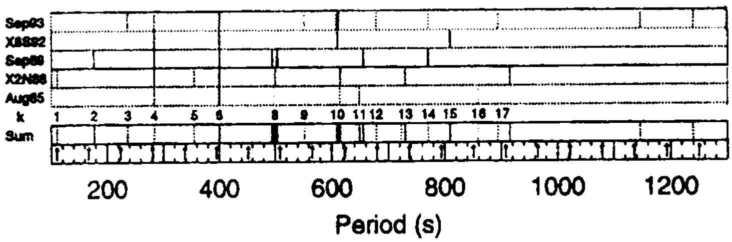

Fig. 2. Schematic diagram of G 29-38's periodicities minus the linear combination modes. The arrows in the bottom panel show where precisely equally-spaced modes would lie.

other seasons also show roughly equally spaced groups, but are often missing one or more k values in between each observed mode. Most notable in this respect are the X2N88, Sep89 and X8 S92 data sets. We now have evidence for a series of successive-k, same-l modes.

1.2. Period spacing analysis

As Fig. 2 readily shows[1] the power spectrum of G 29-38 changes dramatically from year to year. It appears, however, to make its most dramatic changes when the star is behind the sun and we are not watching it. While this predisposition means we do not get to watch the star change, the advantage is that the FT of each individual year provides a relatively stable set of modes that may be used for asteroseismological analysis. In order to have a simple model to compare to our observations (and not get lost in parameter space of purely theoretical model pulsation spectra), I plot in the bottom panel of Fig. 2 a set of equally spaced arrows (the spacing is 57 s) to simulate a series of successive k, $l = 1$ modes. Warning. We are *not* in asymptopia here. We do not expect to see strictly uniform period spacing. Rather, we have identified modes starting at $k = 1$ which is certainly *not* in the high-k limit. Our search for equal period spacing should not be too strict; we expect to see significant departures until we get to the higher-k modes. We also expect deviations on the order of 10 s or so due to mode-trapping effects. In some cases, however, models of Bradley (1995) show deviations of as much as 20 – 30 s.

---

[1] It would be even more obvious were the amplitude information kept in that plot.

Under the assumption that each group is a different k, $l = 1$ mode, I provide a running k assignment for each group as shown in Fig. 2.

The remarkable pattern of Fig. 2 means our initial guess that the linear combination modes were responsible for obscuring the normal mode structure is probably right. Almost half of the observed non-combination modes repeat at least once in the data set; four are present in four of the five data sets. We have indeed uncovered the stable structure underlying all our observations of G 29-38 and now, for the first time, have a hope of making detailed asteroseismological measurements on a DAV.

All the observed modes fit well with an $l = 1$ model and their expected period spacing. The most likely possible exception are the two modes near $k = 17$, but they could also be $k = 17$ and $k = 18$ without much problem. I will therefore consider them as $l = 1$, $k = 17$ and $k = 18$, but to be safe, will offer an alternative explanation of $k = 17$ and something else. Fig. 3 is the corresponding ΔP vs. P diagram in which I have adopted the following assumptions and conventions:

- Each mode in the sum panel of Fig. 2 is the same l (presumably $l = 1$).
- Where obvious multiplets are present, I take either the period of the middle mode (presumably $m = 0$) or the largest amplitude mode where only two members of the multiplet are seen.
- The gap between what we have identified as $k = 6$ and $k = 8$ is a missing mode we will call $k = 7$. I will tentatively plot the spacings for these modes (with dotted squares) as 1/2 the $k = 6$ to $k = 8$ spacing. This is done only to show the mean spacing agrees with the rest of the data. I do the same for the two long-period modes.
- There will be unavoidable uncertainties in the modes' periods (and differences) since the m values are uncertain.
- I use forward differences.

In the interest of completeness, I have plotted some alternative identifications in Fig. 3. With the exception of the two modes near $k = 17$, there is no reason to suspect any of these modes are a different l. On the other hand, there is nothing besides Occam's razor to forbid having a mode or two of a different l. Based on the previous WET observations and the work of Clemens with the hot DAVs, it seems unlikely that the majority of the modes are anything other than $l = 1$. (Evidence from Sections 2 and 3 also supports this conclusion.) However, since it is possible to have a

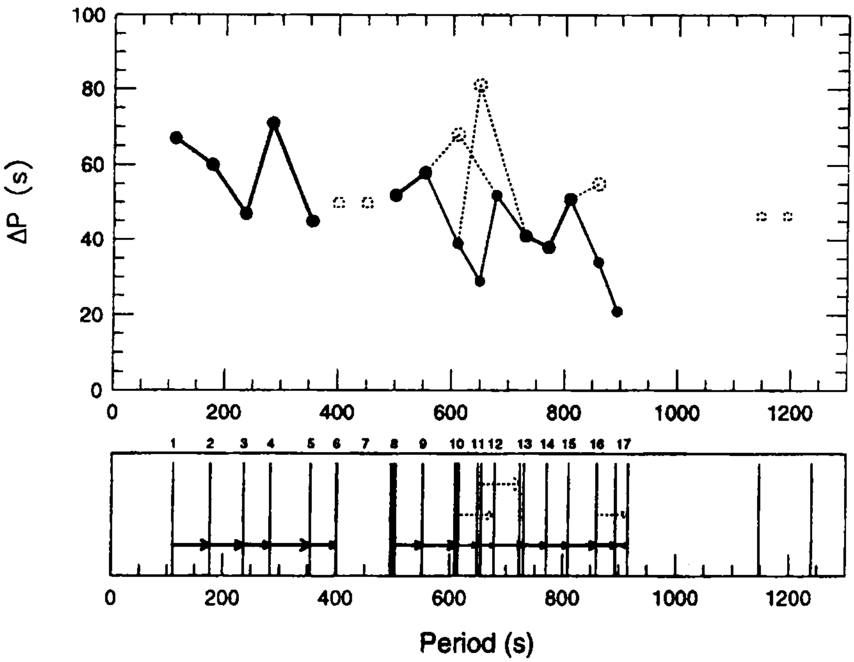

Fig. 3. The observed ΔP vs. P diagram for G 29-38

mode or two of a different-l sneak into our identifications, I have plotted some likely alternatives to the $l = 1$ only model by dotted lines and circles. Where I have plotted such alternatives, the only $l = 1$ interpretation is plotted with thinner lines and slightly smaller filled circles. The bottom panel of the plot is an enlarged plot of the sum row of Fig. 2 with arrows showing which modes were used to calculate the differences shown above it. The line type of each conforms with the convention used in the first panel. Above this plot are k assignments at $l = 1$.

There are few published models for DAVs since until just recently, we have not had many observed modes to test them with. Those models that we do have are almost certainly incomplete since they have not yet been faced with many observational tests. Nonetheless, there are some interesting model comparisons to make. In Section 3, I discuss the cool DAV group modal properties and derive a set of modes common to all the cool DAVs which I use to place constraints on the H-layer of these stars. The advantage of using this subset of modes (the "class modes" of the cool DAVs) is that they are unlikely to be a mixture of l s given the power spectra similarities found in Section 3. The ΔP vs. P diagram for the model fit to these modes is shown in Fig. 4.

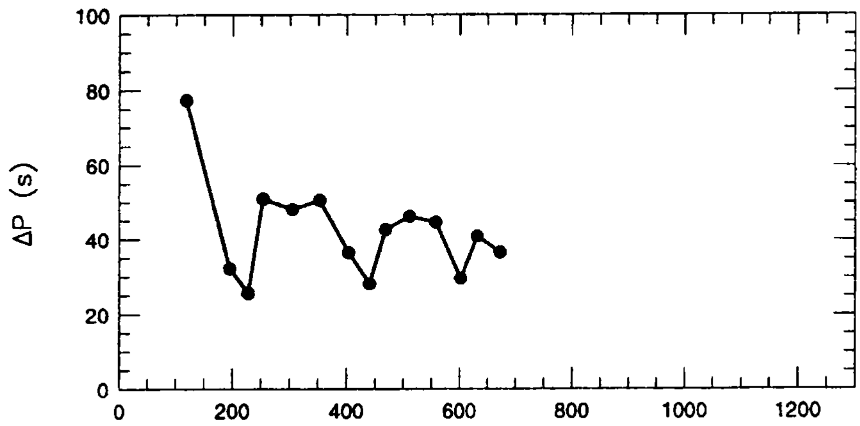

Fig. 4. The ΔP vs. P diagram for a DAV model from Bradley (1995).

The model is not a good fit. More serious than the misalignment of the trapping cycles (as this may be corrected through adjustments of the H-layer and total stellar masses) is the mismatch of the overall shape of the two diagrams. G 29–38's period spacings show a trend which decreases in time, whereas the model has maxima that decrease and minima that increase. That these overall shapes do not agree is no big surprise;[2] this is the first time we have had an observational DAV ΔP vs. P diagram with which to compare the models. The observers have opened the ranch gate – let the theoretical herd out!

1.3. Mass estimates and mode-identification implications

The mean period spacing, P_0, of a set of successive-k, same-l g-modes is a direct function of the stellar mass. No detailed mode calculations of this correlation have been previously published. Bradley

[2] Some might argue otherwise, since the existing models matched the first asteroseismological test put to it, the WET observations of PG 1159-035, incredibly well. I maintain that the success of this match was the surprise. That the DAV models don't exactly match their first critical test this time, I do not find particularly surprising.

(1995, private communication), however, has run some models based on the results of this work. He has assumed a hydrogen layer mass of $10^{-4}\,M_\star$ and finds decreasing the hydrogen layer increases the period spacing significantly. For a $0.6\,M_\odot$ model, for example, P_0 increases by roughly 7 s when the hydrogen layer mass is decreased from $10^{-4}\,M_\star$ to $10^{-6}\,M_\star$. Fig. 5 shows, for a series of model masses, the relationship between π_0 (the theoretician's equivalent of the observed mean period spacing, equal to $P_0\sqrt{\ell(\ell+1)}$) and the effective temperature of the star. Using the temperature of Bergeron et al. (1995) and our measured P_0 (51 s), we can estimate the mass of G 29-38. As shown by the dotted lines in Fig. 3, we get a mass near $0.55\,M_\odot$. Bergeron et al. measure $0.69\,M_\odot$. To get $0.7\,M_\odot$ with our measured period spacing and these models would require a temperature well outside the instability strip – not very likely. The allowable mass range with temperature as a free parameter is about $(0.5\text{–}0.6)\,M_\odot$. To get $0.7\,M_\odot$ using the Bergeron temperature would require lowering P_0 by 10 s, equally unlikely. While there could be missing modes in between those observed, they would skew the uniformity so much, it would no longer look like roughly equal period spacing. To decrease the model π_0 via the hydrogen layer mass would require a larger H-layer mass than already used, making it unstable to nuclear burning. If the modes were $l = 2$, incidentally, the resulting star would be an extremely low- mass object, with a π_0 near 125 s. The majority, at least, of the modes must be $l = 1$.

The mass discrepancy, however, is interesting. It says G 29-38's mass is more near the norm of $0.6\,M_\odot$ than most mass estimators have placed it. G 29-38 historically comes out on the high end of the mass scale. I suggest one of two (or both) things may be the cause:

(1) The asteroseismological models are incomplete. We know this is true from the ΔP vs. P diagram, but the mean period spacing should be less sensitive to model details than are the details of mode trapping.

(2) Something strange is happening to G 29-38's envelope due to its large and highly non-linear pulsations which affect the spectroscopic estimates.

Either way, the field of individual DAV asteroseismology is off and running.

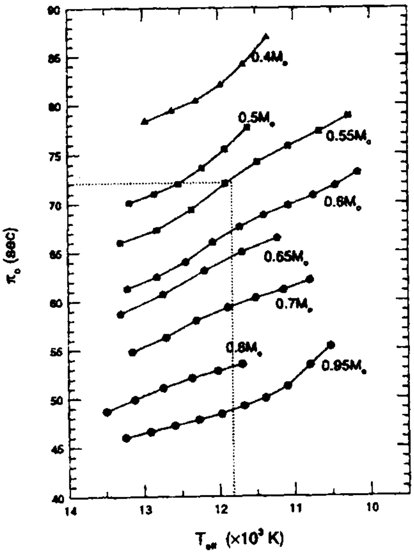

Fig. 5. Model fits of π_0 $(P_0(\ell(\ell+1))^{1/2})$ for a variety of DA masses. The assumed H-layer was $10^{-4}\,M_\star$.

2. G 29–38 multiplets

The observed multiplets on G 29-38 do not quite fit the standard picture. We see two sets of multiplet spacings, but they are not entirely consistent with $l = 1$ and $l = 2$ spacings. We also see multiplet spacings that change significantly from year to year, possibly periodically. Only twice do we see identical multiplet spacings in the same data set.

2.1. The 400 s region

The best example of a rotationally split multiplet in G 29-38 comes from the modes near 400 s (2500 μHz). Unlike most of the other power which comes and goes in each yearly data set, there is always power present in this region. The triplet is nearly evenly-spaced and has an average spacing around 5 μHz. Assuming this is an $l = 1$ triplet, and not 3 components of a higher-l multiplet, the largest-amplitude peak is always the $m = -1$ or $m = +1$ but never the $m = 0$ mode. In some cases, the $m = 0$ mode is not seen at all. The equally-spaced triplet supports the $l = 1$ assignments made earlier.

The observed frequency splitting is not constant from year to year. Fig. 6 is a schematic diagram which shows the position of each multiplet member in each of the yearly data sets. In two cases, the $m = \pm 1$ modes were seen, but not the $m = 0$, so I plot a smaller line segment at the mean of the two observed modes. The data in Oct90 do not have a high enough signal to noise ratio or resolution to detect but one mode, although more may be present, but hidden in the noise.

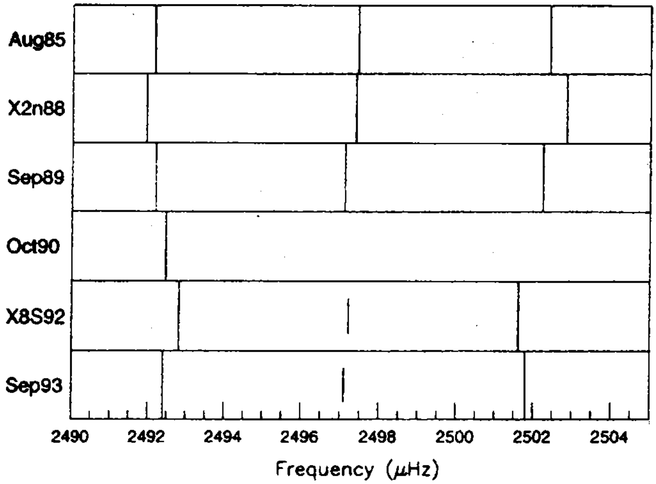

Fig. 6. Schematic diagram of the 400 s multiplet over time.

The central $m = 0$ (or median of the $|m| = 1$) mode remains at roughly the same position, (2497.32 ± 0.17) μHz, based on the three times it was observed. The spacing between the $m = -1$ and $m = +1$ changes by nearly 2.0 μHz (each m moving about 1.0 μHz). Since the changes are nearly symmetric with respect to the $m = 0$ mode (although this is a little uncertain since the $m = 0$ is not always seen), the cause can not be a changing simple magnetic field; it is more like a change in rotation.

Although not yet in the published literature, these sorts of multiplet irregularities are not completely new. During the XCOV10 run on GD 358, we saw severe changes in the multiplet structure both as the run went on and as compared to the previous WET run on the star. During the run, for example, many of the triplets actually

Table 1. G 29–38's 400 s triplet over time

Data set	Frequency (μHz)	Amplitude (mma)	Spacing (μHz)
Aug85	2492.16	4.4	5.28
	2497.44	7.0	
	2502.42	8.8	4.98
X2N88	2491.95	4.9	5.44
	2497.39	4.8	
	2502.85	10.9	5.46
Sep89	2492.268	9.7	4.85
	2497.118	1.3	
	2502.083	4.9	4.97
Oct90	2492.47	8.0	
X8S92	2492.82	11.2	4.40
	2497.22	Average	
	2501.62	4.5	4.40
Sep93	2492.41	6.0	4.68
	2497.09	Average	
	2501.77	5.7	4.68

looked more like quintuplets for a time, but then came back to a triplet state. These changes occurred on timescales as short as a few days. While we cannot apply our explanation of these phenomena to G 29-38 (only because we don't have one), it is worth noting that there is additional evidence for some fundamental flaws in our simple picture of ever-lasting equally-spaced multiplets.

Table 1 gives the frequencies and amplitudes for the triplet in each data set. The average spacing of 4.9 μHz corresponds to a rotation period of 1.2 d. The range of spacings correspond to rotation periods from 1.1 to 1.3 d, assuming that the asymptotic expression for $C_{\ell,k}$ is valid.

2.2 The 284 s mode

Besides the 400 s multiplet, the only consistently recurring area of power in G 29-38 is the 284 s mode, which does not, unfortunately, show similar multiplet characteristics. Only once, in the Sep89 data, is another peak clearly seen in the transform. Fig. 7 shows an additional peak spaced 5.9 μHz to the right of the 284 s mode. In the remaining data sets there are some cases with a slight excess of power near this mode, but it is never conclusive. In Aug85, there is clearly excess power in this region and it is consistent with a multiplet component at the same place as seen in Sep89, but not well-resolved. Since the spacing observed in 1989 is similar, although not equal, to that in the 400 s mode, there is some support for labeling the 284 s mode and the 400 s multiplet as the same l although we still have to account for the slight, but significant, difference in splitting. (Slightly differential radial rotation rates could explain it.)

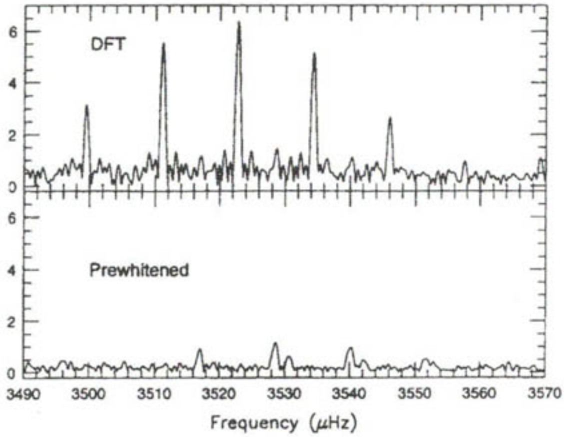

Fig. 7. Fourier transform of the 284 s region of G 29–38 in Sep89.

2.3. The 500 s Region

While not as stable as the 284 s and 400 s regions, there is recurring power near 500 s. The exact periods seen in any given year vary and the region is not always completely resolved. Fig. 8 shows the FT of this region in each of the primary data sets. I conservatively pre-whitened and synthesized the FT and light curve around this region and mark what peaks I believe are real with arrows in Fig. 8. There are no arrows in Sep89 despite there being obvious power there because it is very unclear which modes are real – they are not at all resolved. The Aug85 and X2N88 data sets show fairly obvious triplets with near equal (but different in each data set) spacings. The only identified peak in the Sep93 data set matches the central ($m = 0$) component of these two triplets, but the power seen in the

Table 2. Identified power in the 500 s region of G 29–38's FTs.

Data set	Frequency (μHz)	Amplitude (mma)	Spacing (μHz)
Aug85	1999.84	5.3	6.94
	2006.78	5.7	
	2013.97	3.1	7.19
X2N88	1998.39	7.5	8.51
	2006.91	5.7	
	2015.34	6.2	8.43
Sep89	???		
Oct90	1962.25	1.9	
X8S92	2025.69	2.7	
Sep93	2006.58	6.1	

Oct90 and X8 S92 data sets do not match at all. Table 2 lists the identified frequencies and their spacings.

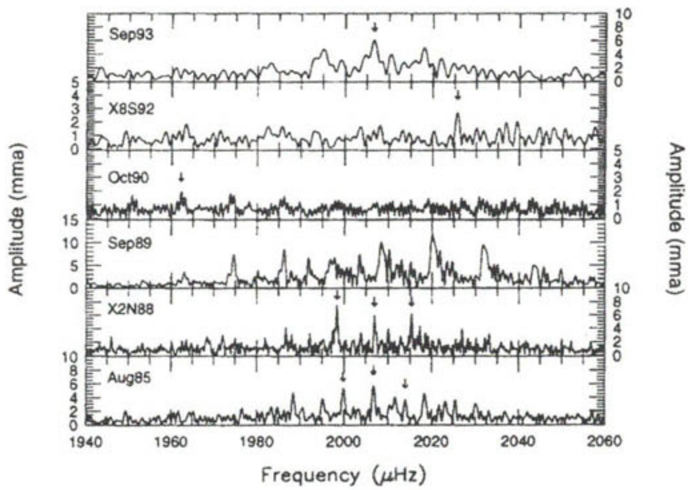

Fig. 8. Fourier transform of the 500 s region in G 29–38 data.

Twice this region has been resolved into a triplet that shows similar behavior to the 400 s triplet. The central $m = 0$ peaks appears to remain stable while the $m \neq 0$ peaks move symmetrically about the $m = 0$ mode. With only two measured spacings, I cannot say quantitatively if the same phenomena are happening here as with the 400 s mode, but I do note the direction of the frequency change from Aug85 to X2N88 is the same as in the 400 s mode, but with a larger absolute (and relative) magnitude. The spacing observed here averages to 7.8 μHz compared to 4.9 μHz for the 400 s modes. If the 400 s and 500 s triplets are the same l, then there must be radially differential rotation in the star. (Models of Bradley [private communication] show $C_{\ell,k}$s that only vary by at most 30 % when not in the asymptotic limit. This is too small a change to be the cause here.) If this splitting represents an $l = 1$ rotationally split mode, the rotation rate is 0.7 d.

The ratio of the average 500 s splitting to the average 400 s splitting[3] is 1.59, close to the expected value of 1.66 for the $l = 2$ to $l = 1$ ratio, suggesting therefore, that the 500 s mode is $l = 2$ and the 400 s mode is $l = 1$. That we only see triplets and not quintuplets cannot rule out an $l = 2$ identification, although it is suggestive. This ratio may, however, just be a coincidence. Taking each season separately, the splitting ratio for Aug85 is 1.38 and for X2N88 it is 1.55. These ratios, which may be more meaningful as they are ratios taken in the same seasonal data set, are not as close to the predicted $l = 2$ to $l = 1$ ratio as the overall average ratio is. The multiple-l explanation does not fit any better.

The modes seen in X8S92 and Oct90 are of low signal to noise, and therefore hard to classify. There is clearly something happening in the Sep89 data set as well, but the data are simply not resolved. There may be instances of both the high (near 8 μHz) and low (near 5 μHz) spacings at once in this data set, but it is very hard to see the forest for the grass.

2.4. The 615 s mode

The dominant power in the X2N88 data was a mode at 615.15 s. Winget et al. (1990) claimed this mode was single, isolated and showed a strange, unexplained phase variation. Their plot of the observed FT and spectral window convincingly shows there are no nearby peaks. However, upon pre-whitening the data by the 615 s mode, I found there is indeed another mode nearby – spaced 8.53 μHz

[3] These are averages of the splittings seen each year.

to the right. The 615 s mode's first harmonic also shows the same structure. Both of these modes are seen in Fig. 9. The 8.5 μHz spacing here is the same as seen in the 500 s triplet in this same data set. The simplest explanation of this mode therefore, is it is the same l as the 500 s modes and at least one component of the multiplet is missing.

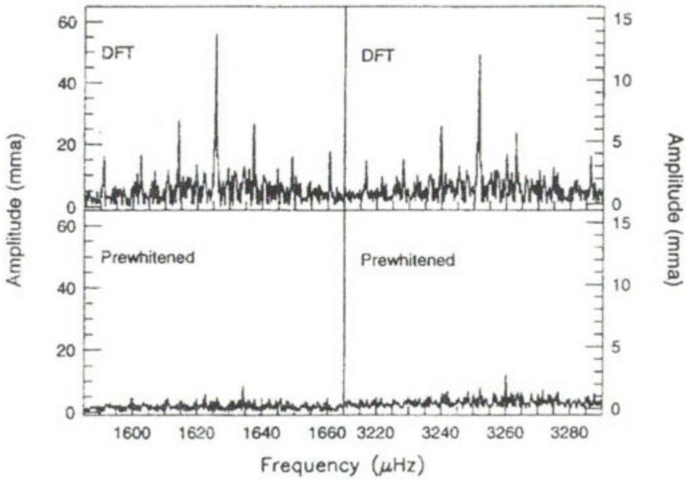

Fig. 9. The 615 s and first harmonic region with the main peak removed from the data (X2N88 data).

The beat period between the dominant mode and this new companion is almost 33 hours, so during a single run the two modes will not be resolved. What effect will this have on the phase of the 615 s mode? Could this previously unseen mode be the cause of the 615 s phase variation? Or could it be an artifact produced by the FT to accommodate the observed (but perhaps real) phase variation?

To answer these questions, I simulated a light curve containing only the two peaks near 615 s and then did a linear least squares (fixed period) O–C fitting only the 615 s mode. The resulting O–C showed no sign of the previously observed variation, proving the new observed mode is neither the cause nor effect of the observed phase variation. Not accounting for this mode's presence had roughly a 10 % effect on the phase of the 615 s mode. Kepler et al. (1995) give a formula for the phase variation caused by an unresolved doublet

$$\tan\phi_{\rm max} = \frac{A_1/A_0}{[1-(A_1/A_0)^2]^{1/2}},$$

where $\phi_{\rm max}$ is the expected phase wander and A_0 and A_1 are the amplitudes of the largest and smallest peaks, respectively.

For these two modes, we expect only a few percent variation in phase and a fairly short beating timescale – slightly over one day. The variation of Winget et al. was over a much longer timescale and had a much larger amplitude.

In 1989, the 615 s mode disappeared, but by the end of the 1992 season, power near there started to reappear. By Sep93, its amplitude had grown to 33 mma and clear multiplet structure emerged. Fig. 10 shows the FT in this region. The frequency spacing this time is 4.7 μHz (as opposed to the 8.5 μHz splitting seen in the X2N88 data) – identical to that seen in the 400 s mode this season, suggesting (if the different splittings are due to different l s) this is the same l as the 400 s mode and different l from the 500 s region. This is in direct contradiction with the two modes found in the X2N88 data which suggest the 615 s power is the same l as the 500 s region and different from the 400 s power. It is possible there is a missing mode in the X2N88 doublet so the spacing is really 4.2 μHz, much closer to that seen in Sep93. It is difficult, however, to call the match between the 8.5 μHz spacing in these two modes and that of the 500 s triplet in the same data set as a coincidence. Figure 11 schematically shows all the main multiplets in each data set and readily shows which multiplets "agree" with each other when.

The 615 s period in the X2N88 data set is roughly 7 μHz away from the nearest peaks seen in Sep93; its companion peak falls right in between the left-most and central Sep93 components. This difference is not easy to explain and suggests we may not be seeing the same normal mode in the star. The phase (or period) of the 615 s peak in the X2N88 data was changing rather dramatically. When nearby power reappeared in 1992 and grew in amplitude through Sep93, its frequency again changed significantly, from about 1638 μHz to 1630 μHz. Given the mode's large amplitude in addition to this frequency change, we suspect there is a strong resonance or trapping here and these two sets of modes are probably the same normal

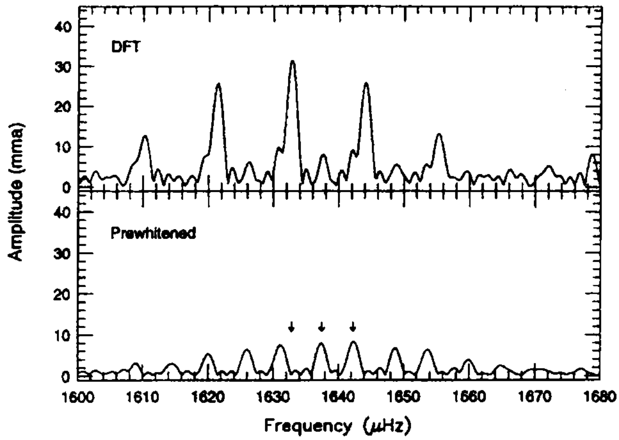

Fig. 10. The Sep93 G 29-38 DFT near 612 s with arrows indicating the multiplet components.

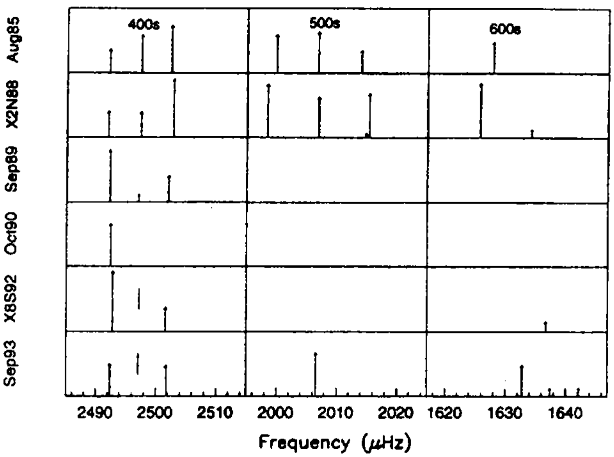

Fig. 11. A schematic plot of all the major observed multiplets. The short line segments are not real modes, but averages of the two flanking modes.

mode of the star[4]. As the mode grows in amplitude, it may be pulled more and more into the trap. We observed the 600 s mode's period increasing as it grew in 1992 to 1994, just in the direction it would need to go to match the larger X2N88 mode. It is also the direction

[4] Actually, this is more than a suspicion. The ΔP vs. P diagram presented in the previous section shows the 615 s mode is near a deep trap.

Table 3. Identified power in the 600 s region of G 29–38's FTs.

Data set	Frequency (μHz)	Amplitude (mma)	Spacing (μHz)
Aug85	1627.85	31.3	
X2N88	1625.73	55.5	8.53
	1634.26	8.6	
X8S92	1638.68	10.6	
Sep93	1632.79	31.6	4.63
	1637.42	8.2	
	1642.21	8.5	4.79

we expect (from the ΔP vs. P diagram of Section 1) trapping to pull the mode. Incidentally, this observation has important implications to mode-trapping. It shows the strength of the trap is proportional to the amplitude of the trapped mode. While this correlation may be intuitive, it is certainly not included in the linear trapping theory and could be used to calibrate non-linear models.

The different m-splittings of the two sets of 600 s modes, however, still remain a problem. This apparent contradiction could be explained in at least two ways (a good theorist, and even many bad ones, can always come up with an explanation after the fact): a change in the (differential) rotation in the star, or the existence of an $l = 1$ and a $l = 2$ mode near 615 s which "take turns" being excited to observable amplitude.

The Aug85 and X8S92 data sets show some evidence of excess power in the 615 s region, but the data are not good enough to resolve it. In Aug85, there is possibly a peak about 9 μHz away from the dominant peak and in X8S92, there is excess power in one of the alias sidelobes of the main peak, split about 2.5 μHz to the left. Table 3 lists all the identified power in the 600 s region.

2.5. Conclusion

There are many other regions in the FTs with excess power, but none that can be unambiguously identified as a multiplet of any sort. The power in the 800 s region, when present, often shows excess power, but is never resolved well enough to say exactly what is going on. So we are left having to explain only the modes already presented.

There are two classes of multiplets seen, both triplets, but with spacings either near 5, or 8 μHz. The 400 s mode is always of the first class; the 500 s of the second (plus some unexplained excess power perhaps) and the 615 s alternately falls into both. The 284 s mode once showed a nearby mode with a slightly larger splitting than seen in the 400 s mode the same year. Only twice are there two modes with the same splitting in the same year: 1) X2N88: the 500 s and 615 s modes (large spacing) and 2) Sep93: the 400 s and 612 s modes (small spacing). There are two possible explanations for these matches.

If we maintain all modes are $l = 1$, then in addition to a time variable rotation rate to explain the 400 s multiplet variability, there must be differential rotation (to provide the two sizes of splittings) which in itself is also time variable (hence the 615 falling into both camps). A nice test to this theory would have been to measure a 615 s splitting in Aug85 (where the 400 s was low and the 500 s, high) or a 500 s splitting in Sep93 where both the 400 s and 615 s were low. In the former case, I would expect the 615 s splitting to be high, and in the latter, the 500 s to be low. Although the current data do not permit such measurements, future data may provide such an opportunity if only the star cooperates and shows the needed multiplets at the same time.

Allowing for $l = 2$ in addition to $l = 1$ modes does not do any better since the splitting ratios are not quite right. We would still have to employ time-dependent differential rotation to get things to work. Another possibility is for the 615 s mode to be near an accidental degeneracy where an $l = 1$ and $l = 2$ each have modes in the same place. As such, if the $l = 1$ mode were excited, the $l = 2$ mode could be as well, or perhaps, could take over and wipe out the $l = 1$ mode. Thus, we could be seeing sometimes an $l = 1$ and other times an $l = 2$. This has the additional benefit of maintaining the period spacing described in the previous chapter, as only the $l = 2$ modes near $l = 1$ modes would be excited thereby leaving the $l = 1$ period spacing relatively intact. Such a mixture of modes could also explain why there is often an excess of power observed which is not easily resolved.

We have now had to resort to time-varying, radially differential rotation, or precise accidental degeneracies to explain the observed multiplet components. While such a model may indeed work, it is starting to become weighed down with modifications and amendments. Measured a new and different multiplet splitting? No problem, we'll just adjust the rotation rate at that radius at that instant in time to account for it. Next. What may be more likely than the uncomfortable set of requirements above, is that there is simply more to this than existing theory considers; we may not fully understand all the components that go into the multiplet structure (in amplitude-space, we already know this is true). While I am loathe to resort to new physics having made an unexplainable observation, the large number of parameters in the current model required for a reasonable explanation makes me equally uncomfortable.

The primary purpose of this study was to further improve the mode identifications made earlier. But like everything in this star, nothing is spelled out exactly as we would have it. While we see only triplets (and not quintuplets, for example), the variable splittings are not easily explained by any simple model. While we could use some $l = 2$ modes in a model to these observations, the fit would be a bit worse than the $l = 1$ only model. It will take some time, and some modelling to sort everything out, but I suspect we will find there are additional parameters not included in our stellar models.

3. Other cool DAV stars

Having successfully explored the period spectra of G 29-38 and noted a few unsolved mysteries along the way, it is now time to look at other, similar stars to see what observed characteristics are specific to G 29-38 and what are universal to the particular subclass of DA pulsators. If G 29-38 is simply a weird duck, producing a model that explains all its behavior merely explains a single star. If, however, there are similar affectations in other stars of the same class, whatever we learn about G 29-38 will teach us about the class of stars to which it belongs, and hopefully, a little bit about how these stars got to where they are in the process. In addition, if there is similar behavior in these stars, we can use each star as an additional source of information, an additional clue to the puzzle.

Clemens (1993, 1994) work, which first made DAV asteroseismology possible, made a bold statement: all DA pulsators are the same; variations in their pulsation spectra are primarily due to variations in total stellar mass, nothing more. In arriving at this conclusion, he studied the hotter DAVs and did not include the cool DAVs in much of the analysis. Here, we have a unique opportunity to test Clemens conclusions with a different sample of stars from the ones he used.

It would have been nearly impossible to obtain as much data on all stars similar to G 29-38 as I did on G 29-38 itself, so I concentrated on only a few, and even then, have much less data on each of them than I do on G 29–38. Nonetheless, the data will show, at least pulsationally, that G 29-38 is not simply a weird duck, despite its unique infrared excess (Zuckerman and Berklin 1987). It will also show that the cool DAVs agree with the result that the hotter DAVs form a very uniform class of objects.

3.1. Long period variability and stability

As a glance through the schematic period diagrams of the first section will indicate, G 29–38's power spectrum varies, sometimes dramatically, from year to year. Correspondingly, there are less dramatic, but nonetheless substantial changes occurring on monthly timescales. The other stars I present here, G 38-29, G 191-16 and HL Tau 76 also show similar changes, but to slightly different degrees. The most dramatic, like the change seen in G 29-38 from the X2N88 to Sep89 sets, is G 191-16 between January and November 1991. My best data set is from November 1990 (Fig. 12) and shows a very large-amplitude ($\approx$ 70 mma) pulsation near 1200 μHz. Data in January 1991, show roughly the same power spectra, but by November that year, the 1200 μHz power had completely disappeared with the largest power, now near 1675 μHz, down by more than a factor of four (two in amplitude) (see Fig. 13). The next data set I have, February 1994, looks very similar to the lower-amplitude states of November 1991 with no indication of the once dominant 1200 μHz power. Power near 2000 μHz remains in the transform each season.

While not quite as dramatic as G 191-16 (mainly because its amplitude was not as high to begin with), G 38-29 showed a set of similar changes. In October 1990 (Fig. 14), the largest power was near 1000 μHz with an amplitude of 24 mma. By December 1993 (the next available data set), the same peaks had an amplitude of 36 mma (Fig. 15). It is clear that this area is not resolved, so part of the problem could be beating between closely-split modes due to rotational splitting. The nightly transforms, however, show consistent peaks near 24 mma in 1990, and wildly varying peaks in 1993, with amplitudes ranging from 18 mma to 75 mma, all for runs about the same length. While this is also evidence of beating,

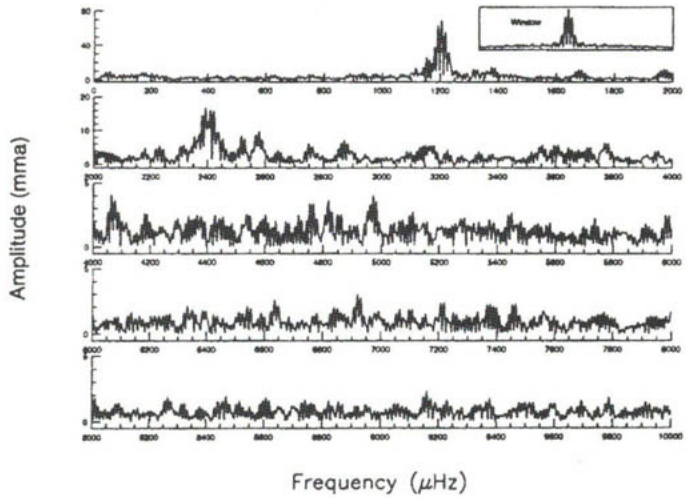

Fig. 12. The FT for the November 1990 data on G 191-16.

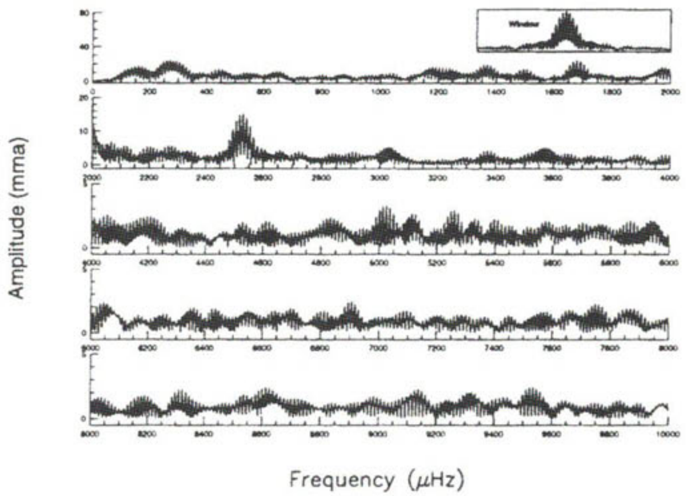

Fig. 13. The FT for the November 1991 data on G 191-16.

the constant 1990 amplitudes suggest a significant change in power during his time period. Further evidence of such change is the power at 1800 μHz absent in 1990, but with an amplitude over 20 mma in 1993. Power near 2000 μHz remains relatively constant.

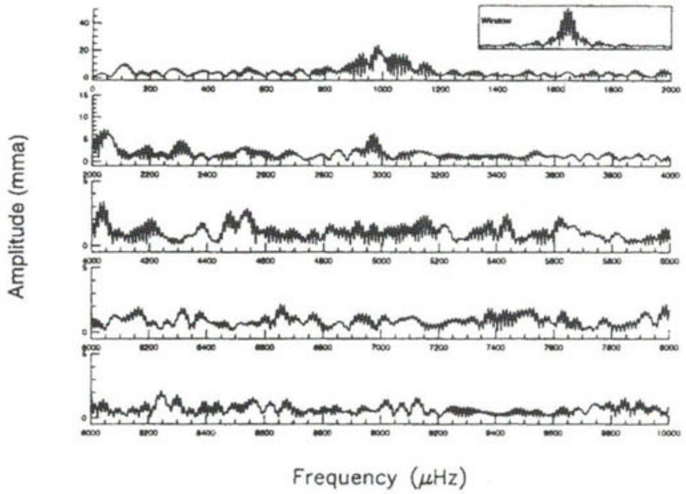

Fig. 14. The FT for the October 1990 data on G 38-29.

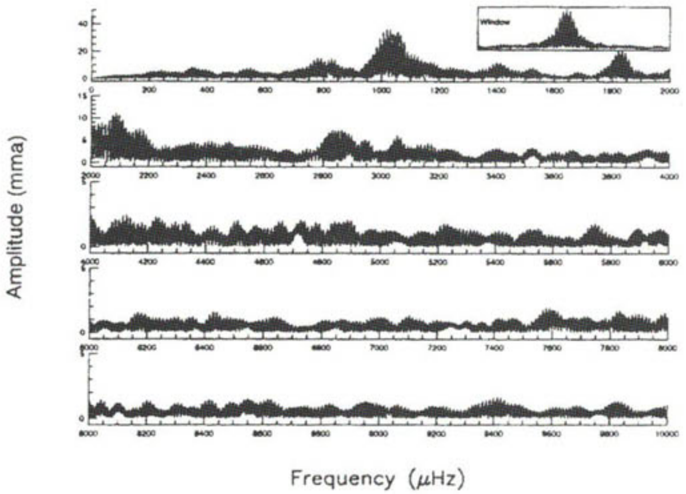

Fig. 15. The FT for the December 1993 data on G 38-29.

HL Tau 76 has power with variable amplitudes near 900 and 1600 μHz. Power at 900 μHz in October and November 1990 is completely absent by February 1991, but reappears in November 1993. While power near 1675 μHz varies from 30 mma in 1990 to near zero in the 1993 data set, it reasserts itself in the following season, January 1992. Powers near 1800, 2000 and 2600 μHz remain present at nearly the same amplitude in all the data sets.

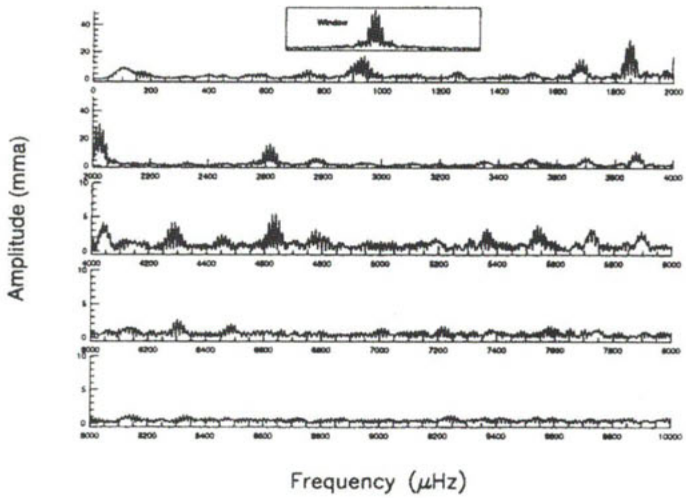

Fig. 16. The FT for the October 1990 data on HL Tau 76.

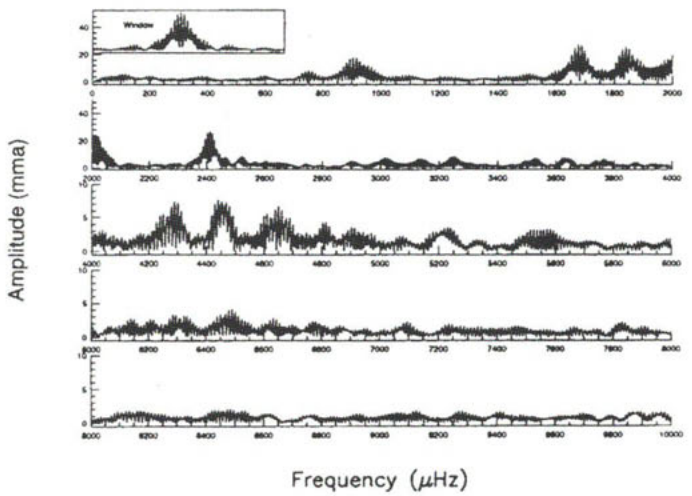

Fig. 17. The FT for the November 1990 data on HL Tau 76.

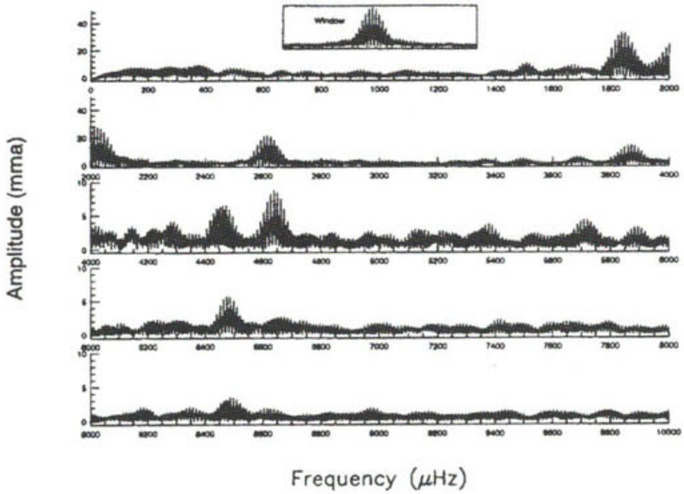

Fig. 18. The FT for the February 1991 data on HL Tau 76.

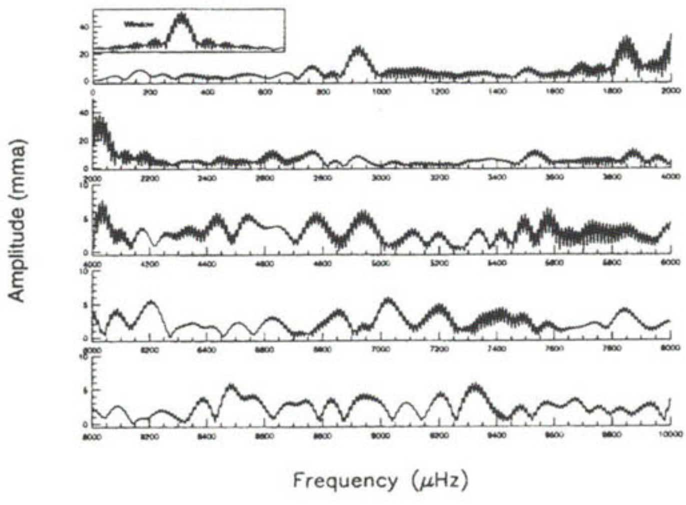

Fig. 19. The FT for the November 1993 data on HL Tau 76.

There is a startling amount of similarity in these stars (and G 29-38). We see very dramatic power changes, modes coming, going and reappearing, and the frequent recurrence of the variable power near 1600 μHz and the stable power near 2000 μHz. Interestingly, all three stars show power near the constant 3523 μHz peak in G 29-38. Unfortunately, the data are not good enough to examine the stability of this mode in these stars, but I suggest future studies may reveal some more interesting clues as to why this particular mode is so stable in G 29-38.

I cannot explain the large power changes and stability observed within them, but I am pleased, nonetheless to find them, for it means time spent studying and understanding any one of these stars will benefit the understanding of all of them. The similarities and differences, I am convinced, will be crucial to exploring their variable nature. It is also encouraging to see power come and go and reappear; it means, with data similar to what we have collected on G 29-38, we can study additional individual DAVs by asteroseismology.

3.2 Class mode structure

With sparse data sets, it is very difficult to identify modes in these complicated pulsators. In addition to signal to noise constraints and rotationally-split multiplet beating, the other major difficulty is the identification and removal of linear combinations. To best avoid these problems, I once again concentrate only on my best data sets: HL Tau 76: October 1990 and G 191-16: November 1990 and November 1991. For the first pass, at least, I don't feel any of the data on G 38-29 are good enough to allow reliable peak identification.

I start, as in G 29-38, by identifying major power in the spectrum, then removing linear combinations as best as possible. and seeing what's left. I have been very conservative and only listed peaks I am sure are real and sure they are not combination modes. In some cases, I have a three mode combination $(A + B = C)$ and know that one mode is real, but cannot determine which of the other modes is real and which is the combination mode (does $A + B = C$ or does $C - A = B$?). In such cases, I left both the uncertain modes out. Even so, there were two modes which I was not completely sure about, but felt strongly enough not to discard them; they are plotted as dashed arrows in Fig. 20 along with the other modes from this analysis. The bottom panel in the figure shows the union of all the modes above it.

Since G 29-38 has many more identified modes than the other stars do, the important thing to see in this plot is if G 29-38 modes exist where there are G 191-16 and HL Tau 76 modes. Indeed, there are obvious groupings at 400, 500, 550 and 600 s with two smaller

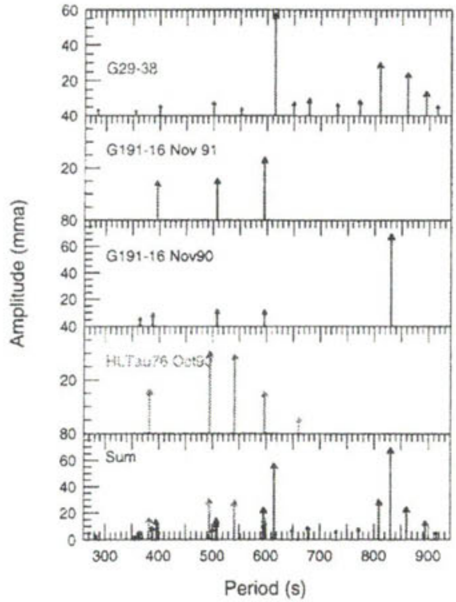

Fig. 20. The non-combination modes of the cool DAVs.

groups at 350 and 650 s. Taken at face value, these groups, with their characteristic 50 s spacing, strongly support the successive k, $l = 1$ identification made in G 29-38. These stars really are very similar. The group widths are between 10–20 s. Even if all the stars had modes in exactly the same place, there would be some natural width to the groups due to the uncertainty of which m-value the modes are. For a characteristic frequency splitting of 10 μHz (corresponding to a rotation period near 0.6 d) the expected widths vary from 3 s for the 400 s group to 7 s for the 600 s group (remember, the spacing is constant in *frequency*, not period). So the groups are only a few times the minimum possible width, given a typical m-splitting.

As Clemens (1993, 1994) showed, there will also be some width to these groups due to the various masses of the stars involved. Ignoring mode-trapping for the moment, increasing the overall stellar mass has two effects: (1) the first ($k = 1$) $l = 1$ mode is at a lower period and (2) the spacing between adjacent $l = 1$ modes will be smaller. The mass of the H-layer, however, also plays a role in the inter-mode spacings. Clemens (private communication) has found the H-layers in the hotter DAs are anti-correlated with mass: the larger the stellar mass, the smaller the H layer, so his observed groups are actually tighter than they would be otherwise. (This correlation is exactly what one would expect for a nuclear-burning based H layer forming mechanism.) With these caveats in mind, I calculated the average of the 400, 500, 550 and 600 s groups and the deviation of each star's modes from the group average. I then shifted each mode of each star by the average deviation. This is different from the method used by Clemens, but justified by the sparsity of modes given the uncertain m-values. The resultant shifted modes are shown in Fig. 21.

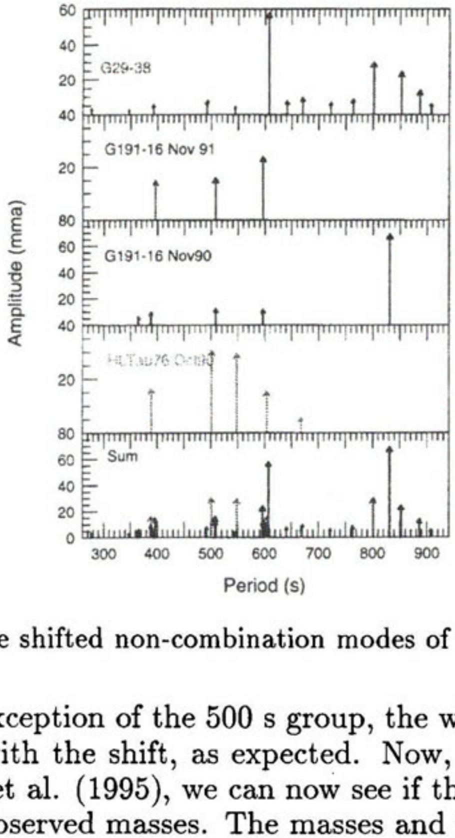

Fig. 21. The shifted non-combination modes of the cool DAVs.

With the exception of the 500 s group, the width of each group has narrowed with the shift, as expected. Now, taking the masses from Bergeron et al. (1995), we can now see if the shifts are consistent with the observed masses. The masses and temperatures from Bergeron et al. are in Table 4. In order of increasing masses, the stars are HL Tau 76, G 191-16 and G 29-38. If things works as they did with the hot DAVs (and as theory predicts), the ordering of applied shifts from smallest to largest should follow the same pattern. In order, the shifts applied were: G 29-38: −8 s, G 191-16: 0.5 s, HL Tau 76: 6.5 s. The shifts are in precisely the *wrong* order. This result is certainly unexpected and suggests that either first order shift (versus a change in scale due to a changing mean period spacing) is not enough, or the group widths are dominated by m-splitting and not by any effects due to changing mass or composition. Hopefully, more precise model-fitting attempts, which will yield both the overall mass and H-layer mass, and better data which can resolve the multiplet splitting will shed some light on this mystery.

Table 4. Masses and temperatures of the cool DAV's from Bergeron et al. (1995).

Star	Temperature (K)	Mass ($M_\odot$)
G 29–38	11820	0.69
G 191–16	11420	0.64
HL Tau 76	11440	0.55
G 39–29	11180	0.55

3.3. Model fits

The average of the four observed groups are 390 s, 500 s, 547 s and 603 s. For an average period spacing (between successive $l = 1$ modes) of 50 s, these periods are consistent with a series of consecutive-k (save 1) [6] $l = 1$ modes. If so, it would be nice to see what the pulsation models, which have proven so successful for PG 1159-035 and GD 358, say about the structure of a star with these modes.

After Clemens's work on the hot DAVs, Bradley (1995) published a set of DAV models with thick (near $10^{-4}\,M_\star$) H-layers. Previously, Bradley (1993) had already published models with thinner H-layers, from 10^{-5} – $10^{-13}\,M_\star$. I will first take the average star (a fictional star with modes at the group averages) of average mass ($0.6\,M_\odot$) at a temperature near 11 750 K (where Bradley's grids are calculated and quite close to the observed temperatures of Bergeron as well) and see what constraints can be placed on the H-layer mass.

For this fictional mass of $0.6\,M_\odot$, there are two models that fit reasonably well: one with a $10^{-4}\,M_\star$ H-layer and one with a $10^{-9}\,M_\star$ H-layer. The model fits are summarized in Table 5.

[6] The missing mode, presumably near 450 s, is the same mode missing in the G 29-38 data. What is this telling us about the stars' common structure?

Table 5. Bradley (1993, 1995) $\ell = 1$ model fits to fictional $0.6 M_\odot$ cool DAV.

Observed period (s)	$M_H = 10^{-4}\, M_\star$ Period (k) (s)	$M_H = 10^{-9}\, M_\star$ Period (k) (s)
390	406 (6)	419 (4)
500	493 (8)	502 (6)
547	538 (9)	540 (7)
603	599 (10)	610 (8)

Clearly, neither model is an exact fit, but given the coarseness of the search grid, both are good indications that a more exact fit could be found with suitable parameter adjustment. Unfortunately however, based on this model star alone, we cannot distinguish well between the thick and thin H-layer cases. Using the individual stars, with their own periods and Bergeron et al. masses, however, may help limit our choices.

Starting with G 29-38, I can find no thin layer models from Bradley (1993) that can match the observed group modes. Amongst the thick H-layer choices, a model with a $1.0 \times 10^{-4}\, M_\star$ layer is the best fit with a $1.5 \times 10^{-4}\, M_\star$ layer a close second. The model match is in Table 6. The fit is quite good and could certainly be improved by using more modes and a finer grid in parameter space.

Table 6. Bradley (1995) $l = 1$ model fit to G 29-38 group modes.

Observed period (s)	Model period (k) (s)
355	353 (6)
400	403 (7)
500	511 (10)
552	557 (11)
609—615	602 (12)

Matching models to HL Tau 76 and G 191-16 present a little more of a challenge, only because the Bradley (1995) grids are not very complete for modes with their masses (0.55 and 0.65 $M_\odot$) and the thin layer Bradley (1993) models do not cover these masses at all. Nonetheless, one can get reasonable fits in the thick layer range of 10^{-4} for HL Tau 76, the least massive of the two, and 10^{-5} for G 191-16. If two can be called a trend, this trend of thinner H-layers with increasing mass agrees with what we expect. G 29-38, however, with its higher mass should have the smallest H-layer, but it has one of the largest, instead. Perhaps this is tied in with G 29-38's other peculiarities, or perhaps it is just highlighting the tentative nature of these model assignments. Or, given the incompleteness of the lower-mass models, we may be seeing a correlation of the H-layer with overall mass opposite that seen by Clemens. If so, the dominant H-layer determining mechanism may still be nuclear burning, but winds, which would decrease the H-layer for less massive white dwarfs, may also play a significant role.

The important thing to come out of this search through model space is that these results, based only on the observed groupings of three cool DAVs are consistent with the results of Clemens on the hotter DAVs. All the DAVs, now, are consistent with thick H-layer masses. Once further observations and models arrive, we'll be able to explore these points in more detail, but for now, a direction is indicated, and there is no reason to concentrate solely on thin H-layer models any more. We have provided an independent sample of DAVs from the Clemens sample and get the same result.

Acknowledgments. This work is part of my dissertation work in Texas. As such, I would like to thank my advisors, Ed Nather and Don Winget for their help and support. I am indebted to Darragh O'Donoghue and Don Kurtz for the August 1985 G 29–38 data set which they initially gave me for a purpose different than I am now using it. I would also like to express my thanks to Paul Bradley for quickly running some DAV models to compare with my data.

References

Bergeron P. et al. 1995, ApJ, 449, 258
Bradley P.A. 1993, Ph.D. Thesis, University of Texas, Austin
Bradley P.A. 1995 ApJ, in press
Clemens J.C. 1993, Baltic Astronomy, 2, 407

Clemens J.C. 1994, Ph.D. Thesis, University of Texas, Austin
Kepler S.O. et al. 1995, these proceedings
Winget D.E. et al. 1990, ApJ, 357, 630
Zuckerman B., Becklin E. E. 1987, Nature, 330, 138